

Development of a 15-Degree-of-Freedom Bionic Hand with Cable-Driven Transmission and Distributed Actuation

Haoqi Han, Yi Yang, Yifei Yu, Yixuan Zhou, Xiaohan Zhu, Hesheng Wang, *Senior Member, IEEE*

Abstract—In robotic hand research, minimizing the number of actuators while maintaining human-hand-consistent dimensions and degrees of freedom constitutes a fundamental challenge. Drawing bio-inspiration from human hand kinematic configurations and muscle distribution strategies, this work proposes a novel 15-DoF dexterous robotic hand, with detailed analysis of its mechanical architecture, electrical system, and control system. The bionic hand employs a new tendon-driven mechanism, significantly reducing the number of motors required by traditional tendon-driven systems while enhancing motion performance and simplifying the mechanical structure. This design integrates five motors in the forearm to provide strong gripping force, while ten small motors are installed in the palm to support fine manipulation tasks. Additionally, a corresponding joint sensing and motor driving electrical system was developed to ensure efficient control and feedback. The entire system weighs only 1.4kg, combining lightweight and high-performance features. Through experiments, the bionic hand exhibited exceptional dexterity and robust grasping capabilities, demonstrating significant potential for robotic manipulation tasks.

Index Terms—Biomimetic and bio-inspired robotics, Mechanisms, Hand Design, Tendon driven

I. INTRODUCTION

THE development of actuator systems with human-level dexterity presents significant challenges [1], [2], stemming from the bio-integrated nature of the human hand: it is not an isolated entity but a highly coupled system intricately connected through skeletal-muscular-neural networks to the forearm, forming a synergistic functional unit. This

Manuscript received Month xx, 2xxx; revised Month xx, xxxx; accepted Month x, xxxx. This work was supported in part by the Natural Science Foundation of China under Grant 62225309, U24A20278, 62361166632, U21A20480 and 62403311. (Corresponding Author: Hesheng Wang)

Haoqi Han is with the Department of Computer Science and Engineering, Shanghai Jiao Tong University, Shanghai, 200240, China (e-mail: hhq123@sjtu.edu.cn).

Yi Yang is with the Department of Engineering Mechanics, Shanghai Jiao Tong University, Shanghai, 200240, China (e-mail: yangyi04@sjtu.edu.cn).

Yifei Yu is with the Department of Automation Engineering, Shanghai University of Electric Power, Shanghai, China (e-mail: yuyifei@mail.shiep.edu.cn)

Yixuan Zhou, Xiaohan Zhu are with the Department of Automation, Shanghai Jiao Tong University, Shanghai, 200240, China (e-mail: yixuanzhou@sjtu.edu.cn, zxh_2001@sjtu.edu.cn).

Hesheng Wang is with the Department of Automation, Key Laboratory of System Control and Information Processing of Ministry of Education, Key Laboratory of Marine Intelligent Equipment and System of Ministry of Education, Shanghai Engineering Research Center of Intelligent Control and Management, Shanghai Jiao Tong University, Shanghai, 200240, China (e-mail: wanghesheng@sjtu.edu.cn).

Manuscript received March 1, 2025; revised August 16, 2025.

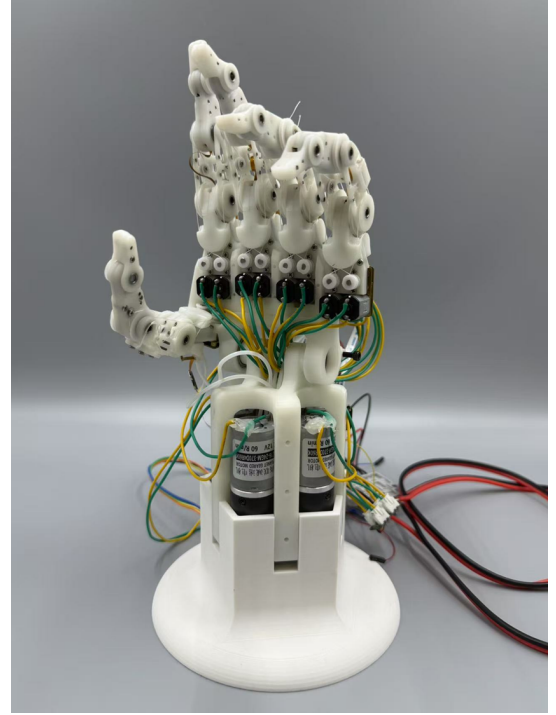


Fig. 1. The IRMV Hand

anatomical architecture enables both high-power grasping and fine manipulation with sub-millimeter precision. Furthermore, the human hand exhibits multimodal sensing capabilities for force, temperature, and texture discrimination, demonstrating exceptional environmental adaptability and task generalization. This demands biomimetic actuators to simultaneously achieve kinematic dexterity, power density, and proprioceptive integration within constrained volumes, creating a characteristic trilemma in mechatronic system design.

The motion of the human finger is primarily defined by the MCP (metacarpophalangeal), PIP (proximal interphalangeal), and DIP (distal interphalangeal) joints. The movements of the PIP and DIP joints are relatively straightforward, typically driven by the coordinated action of the extensor muscles, deep flexor muscles, and superficial flexor muscles, with these movements often being coupled. In contrast, the MCP joint involves more complex motions, such as abduction and adduction, which are controlled by the interosseous muscles, lumbrical muscles, and both the deep and superficial flexors.

Biomimetic finger width design presents a fundamental challenge. Universal human devices strictly adhere to hand anatomical dimensions: the proximal phalanx width measures 16.4 ± 1.4 mm for adult males and 14.8 ± 1.2 mm for females. This dimensional constraint directly governs interaction object design:

- 1) **Precision tools:** Pen barrel diameter (7–11 mm), USB-A connector (12 mm), occupying 40%–60% of human finger width to optimize the compromise between tactile perception and frictional control
- 2) **Grasping objects:** Tool handle diameter (20–35 mm), dumbbell grip (28–32 mm), constituting 10%–20% of proximal phalanx length (72.0 ± 8.0 mm in males), achieving co-optimization of ergonomic comfort and payload capacity under minimal moment arms

In addition, dexterity is a central focus in the development of bionic hands for robotic manipulation tasks. The degrees of freedom in a bionic hand are crucial for enabling complex operations. For instance, to rotate lightweight objects at arbitrary angles within the palm, a bionic hand requires at least four sets of two-link systems, each necessitating a minimum of 3 DOF. Moreover, for grasping tasks, the flexion of the bionic hand's fingers must be capable of delivering substantial power output. This requires at least 12 DOF to meet basic operational requirements.

The rapid evolution of dexterous manipulation research in recent years has demonstrated the potential of high-DoF bionic hands in human-like operational tasks [4]. However, predominant designs with average finger widths ≈ 30 mm constrain demonstration objects to model props. While such validations confirm algorithmic feasibility, they fail to achieve physical interaction with human-centric devices. Consequently, compressing key dimensions of bionic hands to anatomically matched ranges while preserving equivalent kinematics, thereby enabling universal operation of human tools, constitutes a critical technical challenge in the field.

In the design of bionic hands, cable-driven mechanisms offer more flexible configurations. There are generally two types of cable-driven bionic hands: tendon-driven and independently actuated. The tendon-driven bionic hand uses multiple motors to collaboratively drive the finger joints, employing cables to mimic the way muscles drive the skeleton. However, this approach increases the size of the device. In contrast, the independently actuated bionic hand uses a separate motor for each joint, matching the number of joints, which simplifies the transmission structure.

For actuators, the efficiency is typically conserved. When a bionic hand is required to perform both grasping and manipulation tasks, larger actuators are necessary, which inevitably increases the size. However, bionic hands are generally expected to be lightweight and agile, and overly heavy drive systems contradict this goal. To address this, we adopt a distributed drive system design: a cluster of smaller motors is placed in the palm to assist with manipulation, while the core force needed for grasping is provided by a forearm motor. This design balances the demands of grasping and manipulation tasks while preserving the lightness and agility of the bionic hand.

This paper proposes a design for a fully actuated bionic hand, as shown in Fig. 1. The main feature of this design is its distributed drive system, with 10 motors for manipulation mounted in the palm and an additional 5 motors located in the forearm. Additionally, we introduce a novel single-finger, three-degree-of-freedom parallel transmission mechanism, which simulates human hand movement with advantages such as simplicity and a wide working range. To ensure performance, corresponding sensors and motor driving circuits are designed. The main features can be summarized as follows:

- 1) **Distributed Drive Design:** Motors are distributed across the forearm and palm, optimizing spatial utilization and creating a more compact structure.
- 2) **3-DoF Tendon Transmission Mechanism:** A highly efficient parallel tendon transmission design enhances both transmission efficiency and motion flexibility.
- 3) **Bionic Hand Hardware System:** A new hardware system has been developed to achieve efficient motion control and precise operation of the bionic hand.

The rest of this paper is organized as follows: Section II introduces mainstream technical approaches for anthropomorphic bionic hands. Section III discusses the mechanical transmission system of the bionic hand, the distribution of power sources, and the design methods for control circuits. Section IV analyzes the kinematics, dynamics, and working space of the bionic hand, and presents its control principles. Section V presents experimental results demonstrating the bionic hand's performance in grasping tasks. Finally, the paper concludes with a summary of the proposed design and future research directions.

II. RELATED WORKS

For a long time, humans have sought to replicate the physiological structure of the human hand, aiming to develop bionic hands for use in fields such as service, industry, and rescue operations. These bionic hands provide efficient alternatives to relieve humans from repetitive labor or hazardous environments. However, designing a fully dexterous bionic hand presents a significant engineering challenge. The human hand's functionalities, including individual finger movement, grasping, oppositional configuration changes, and tactile perception, require integration of various transmission mechanisms, actuators, and motion sensors. Additionally, challenges related to spatial arrangement, energy efficiency, and control systems must be addressed.

Current approaches to building such bionic hands include module-driven mechanisms, linkage-driven mechanisms, and tendon-driven mechanisms. Each approach has distinct advantages and challenges: direct-drive motor systems offer rapid response but are bulky; linkage-driven mechanisms provide stability but are complex; tendon-driven systems are flexible and lightweight but require high-quality materials and precise control.

1) *Module-Driven:* The module-driven mechanisms is one of the most effective methods for constructing bionic hands, where servo motors are directly integrated within the fingers. This approach offers several benefits, including simplified

design, ease of maintenance, and stable control. Representative designs include the KITECH Hand [5], [6], Allegro Hand [7], Leap Hand [8]. However, direct integration of servo motors in the fingers increases motion inertia, compromising dynamic response and flexibility. Additionally, limited space within the fingers restricts the power output, hindering performance in grasping and manipulation tasks. On the other hand, module-based biomimetic hands typically exhibit substantial dimensions, with an average finger width of approximately 30mm. This necessitates the use of larger-than-conventional objects during operational demonstrations—objects that exceed the size range typically manipulated by human hands. Thus, this method faces challenges in achieving high performance and compact design.

2) *Linkage-Driven*: To enhance the compactness of the bionic finger, the power source is often positioned in the palm or forearm, reducing the finger's size and weight. However, this design increases transmission system complexity, often requiring gears, linkages, or tendon-like mechanisms for power transmission [9]–[11]. For example, the ILDA bionic hand [12] uses a linkage or gear-driven mechanism, offering stability and reducing finger motion inertia. Despite these advantages, linkage or gear mechanisms are not well-suited for long-distance or complex transmission tasks. Consequently, while finger size and weight are optimized, the motor system must still be integrated into the palm, where limited space restricts layout and power output, complicating the balance between force and speed, thus limiting high-performance applications.

3) *Tendon-Driven*: The tendon-driven bionic hand can replicate human hand motion patterns, providing enhanced manipulation and grasping capabilities [13]. By using synthetic fiber rope, the tendon-driven system can perform complex motion synthesis. Its transmission flexibility allows the power source to be mounted on the robot's forearm, reducing the size and weight of the fingers. While this design results in a larger overall volume compared to direct-drive or linkage/gear systems, it offers significant advantages in power output and motion flexibility at the finger level. The tendon-driven system enables higher force output and more precise task execution, making it an effective solution for high-performance bionic hand development. Examples include the Shadow Hand, which features 25 movable joints and 20 degrees of freedom, powered by 20 integrated motors and a cable-driven system [14]. The DLR Hand mimics human hand movement with 19 degrees of freedom, using antagonistic motors and synthetic tendons for a highly realistic model [15]–[19]. The Robonaut 2 Hand, developed by NASA, combines DC motors and synthetic tendons to replicate human anatomy, allowing for tool manipulation in space [20]. The UB Hand from the University of Bologna employs a spring-based structure to replicate finger flexion, offering a simplified but efficient design [21], [22]. Lastly, the FLLEX Hand uses 3D printing and flexible materials to create a robust three-degree-of-freedom hand, capable of high fingertip forces, though its performance in finger extension is limited by the spring mechanism. [23] These developments demonstrate the growing potential of bionic hands in high-precision fields.

However, despite the clean and organized design of inte-

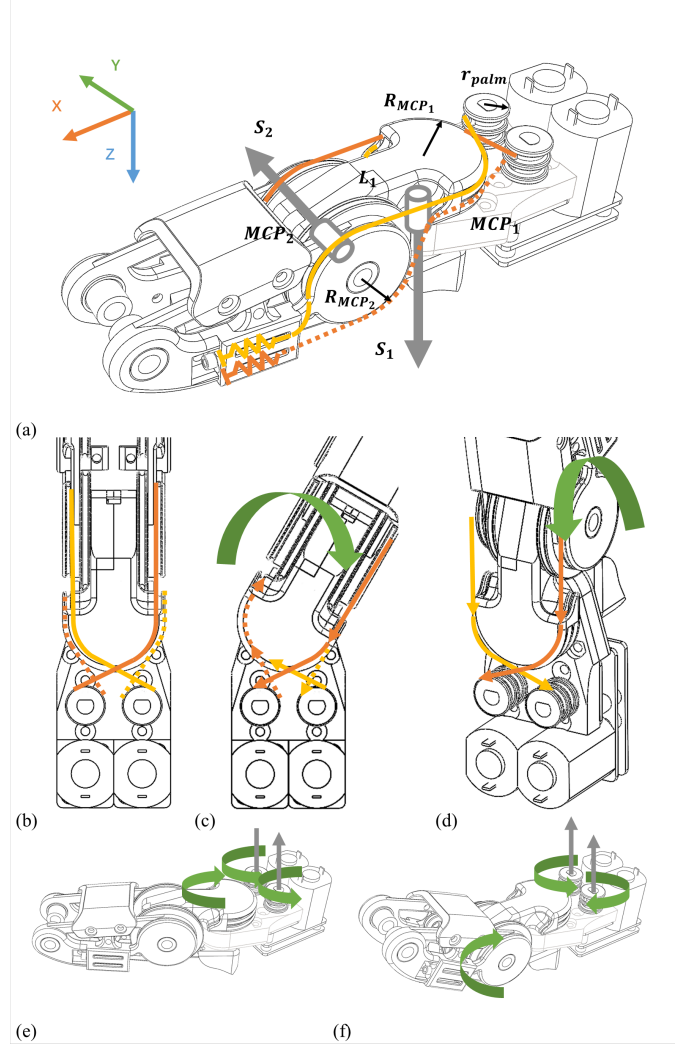


Fig. 2. (a) Structure of MCP joint incorporating spring pre-tensioning mechanisms to compensate tendon slack (springs mounted at tendon termini). Dashed lines denote extension tendons, solid lines indicate flexion tendons; (b) Axial projection of MCP transmission structure, where each pulley module outputs two antagonistic tendons; (c)(e) Simultaneous counterclockwise rotation of dual motors causes synchronous contraction of the left antagonistic tendon pair, generating rightward deflection moment at MCP joint; (d)(f) Antagonistic motor rotation increases tension in solid tendons while decreasing dashed tendon tension, producing adduction moment at MCP joint.

grating motor systems in the forearm, this solution presents challenges in practical applications, particularly for humanoid robots [22], [24]. The large gripping force relies on forearm muscles for power support, while fine manipulation is achieved through precise control in the palm. Therefore, bionic hand design must balance force output with flexibility, integrating forearm power sources and palm precision for efficient, multifunctional performance. This layered drive design not only more closely resembles the physiological structure of the human hand but also provides a feasible solution for practical bionic hand applications [25], [26].

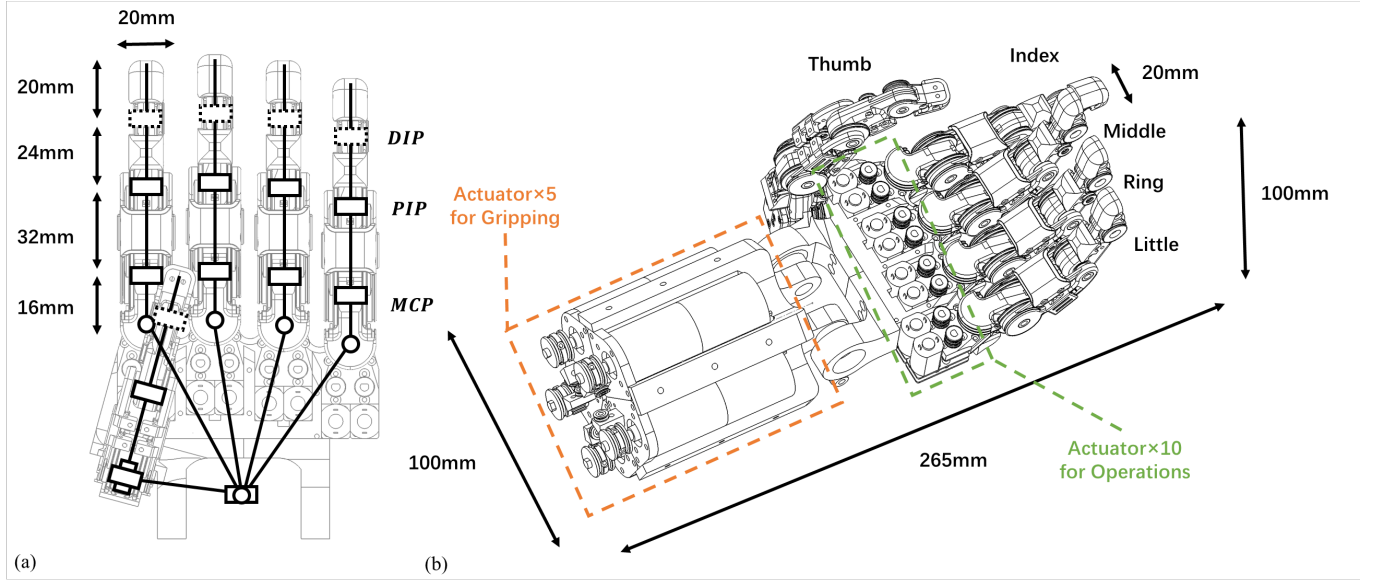


Fig. 3. CAD design of the IRMV Hand. (a) illustrates the kinematic structure of the IRMV Hand, which possesses 15 DOF, similar to the DOF of a human hand. The DIP joint's DOF can be configured as either fixed or active based on requirements. (b) shows the overall structure of the IRMV Hand, with dimensions of approximately $100\text{mm} \times 100\text{mm} \times 265\text{mm}$ and a finger width of 20mm, closely resembling the size of an adult human hand. The forearm section houses five motors for driving grasping functions, while the palm section incorporates ten motors for assisting operational tasks.

III. DESIGN

A. Mechanics

As shown in Fig. 2, the MCP joint's motion is designed with two separate and orthogonal rotational axes. This configuration facilitates the design of a precise cable-driven mechanism and supports a high-load-bearing structure. To address the transmission of the MCP joint, we developed a parallel cable-driven system, utilizing two motors to control its motion. The motors are mounted in the palm, mirroring the anatomical structure of a typical human hand. Each motor's output shaft is connected to a bi-directional pulley, controlling cables for both clockwise and counterclockwise motion. During finger abduction/adduction, bilateral coupled motors rotate synchronously: the left motor tensions solid-orange tendon while relaxing dashed-orange tendon, with the right motor executing identical actions to drive the MCP1 joint toward rightward deflection. Conversely, when the motors rotate in opposite directions, the MCP2 joint performs finger flexion or extension. Additionally, the transmission cables mounted on the forearm pass through the MCP2 joint, providing support to the joint.

In the human hand, the movements of the PIP and DIP joints are typically coupled. In this work, we have developed decoupled motion for the PIP and DIP joints. As shown in Fig. 4, the cable driving the PIP joint passes through a pulley on the second MCP joint and terminates at the middle phalanx. Similarly, the cable driving the DIP joint follows a similar path, terminating at the distal phalanx. Both cables are routed through a conduit connected to the base of the finger, entering the forearm, and are controlled by motors located in the forearm. Since most bionic hand tasks only require actuation of the PIP joint, this design incorporates a dedicated actuation system for the PIP joint, while the DIP joint remains fixed. Critically, the preceding kinematic description represents

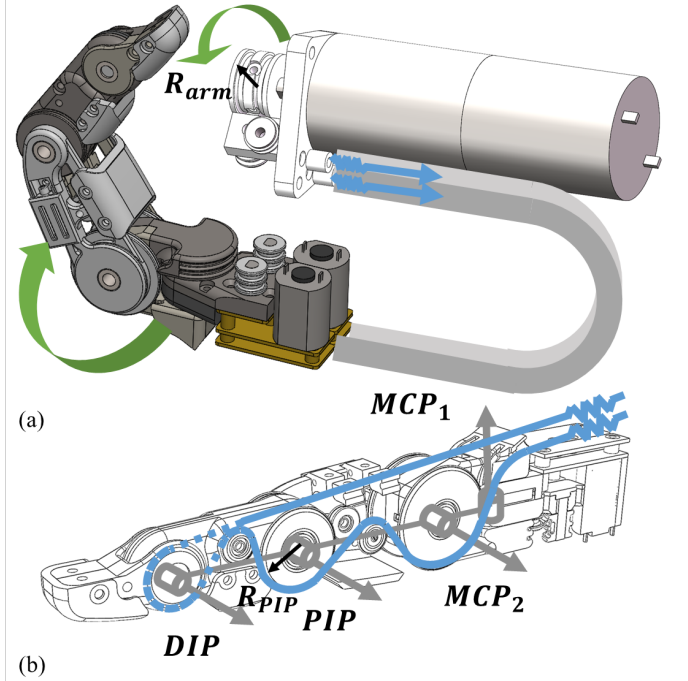


Fig. 4. (a) Kinematic actuation of the PIP joint is driven by motor units located in the forearm compartment, achieving low-friction tendon force transmission via PTFE-lined conduits; (b) Tendon routing configuration for finger flexion and extension motions, generating directed moments at the MCP2 and PIP joints respectively

specific operational cases. Flexion-extension and abduction-adduction motions across all joints achieve full decoupling control by computing motor target tensions from desired joint torque.

This work utilizes DC motors as actuators, employing

motors with varying power to meet the different drive requirements of the bionic hand. The MCP joint is driven by a small motor (N20) located in the palm. For grasping tasks, a higher-power motor (CHR-GM20-180) is employed, mounted in the forearm. In independently actuated bionic hands, transmission slack is a critical issue. To address this, a spring mechanism is positioned at the end of the cable to maintain tension during operation. The spring tensioning mechanism of the palm motor is located at the proximal phalanx, while that of the forearm motor is placed on the inner side of the forearm.

The developed bionic hand exhibits similar dimensions and actuator distribution to those of an average adult male hand. For a complete single finger, the length of the first phalanx is 20mm, the second phalanx is 24mm, and the third phalanx is 32mm. The distance between the two MCP joints is 16mm, resulting in a total finger length of 92mm and a width of 18mm. The five fingers feature the same mechanical structure and are arranged in a manner similar to that of a human hand, with the thumb positioned horizontally. A total of 15 degrees of freedom have been designed, with 15 motors working in tandem to fulfill most manipulation and grasping tasks. The final constructed bionic hand has an overall length of approximately 265mm and a width of about 100mm.

In this work, we adopt an independently actuated approach, combined with the concept of distributed driving, to design a cable-driven bionic hand. As showed in Fig. 3, the hand features five fingers, each with 3 degrees of freedom, aimed at mimicking the muscle distribution of the human hand while effectively reducing the overall structural size. The overall parameters of the IRMV Hand are described in Table I.

TABLE I
MECHANICAL AND ELECTRONIC SPECIFICATIONS OF THE IRMV HAND

Quantity	Value
Number of fingers	five fingers
Finger Degree of freedom	3 DoF
Hand Degree of freedom	15 DoF
Dimension	265 mm × 100 mm × 100 mm
Total weight	1.4kg
Communication	USB

B. Electronics

The control of a bionic hand system is a complex task that necessitates the stable operation of multiple motors and sensors. In most control tasks, force control methods enable more detailed feedback on the interaction with objects. The task will include torque control information for each finger joint, along with corresponding position feedback.

The hardware system of the IRMV hand is shown in Fig. 5. The IRMV hand employs five position sensor boards and four motor driver boards, with the STM32F411 selected as the central controller. Communication with peripheral devices is established via two SPI channels, and the system is controlled by the host computer through a virtual USB serial port. The overall data communication frequency is set at 50Hz, allowing for the collection of position data and the control of motor currents to regulate the bionic hand's output position.

The central controller will reconfigure the sensor and drive interfaces for each finger, encapsulating them into torque control and position feedback for the respective finger joints.

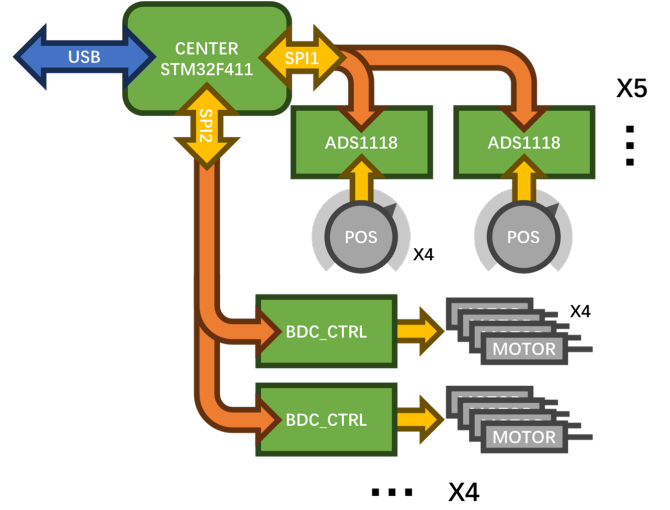


Fig. 5. Hardware system of the IRMV Hand.

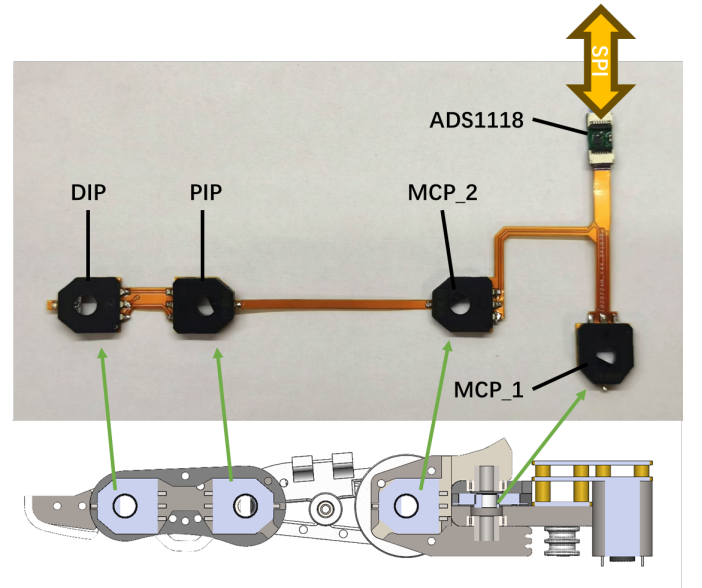


Fig. 6. Position sensing circuit of the IRMV Hand.

To determine the joint angles of the bionic hand, each finger is equipped with four position sensors, totaling 20 sensors. Position sensing is achieved using commercial rotary potentiometers (SV01A103AEA01R00), connected via FPC flexible printed circuit boards and installed internally in each finger. An ADS1118 is placed at the base of each finger for data acquisition, with a maximum joint position sampling rate of 200Hz. The ADS1118 analog-to-digital converter features a 16-bit ADC resolution, enabling the finger joints to achieve an angular resolution better than 0.02°. This part is shown in Fig. 6.

Due to the large number of motors, we designed separate motor control boards (Fig. 7) to ensure stable and high-speed

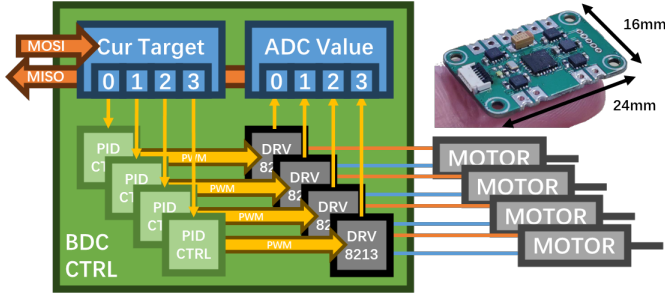


Fig. 7. Brushed Motor Control Board of the IRMV Hand.

control of multiple motors. The motor driver board uses the STM32G071 as the main controller and the DRV8213 for motor driving. The control board operates at a frequency of 64 MHz and employs pulse width modulation (PWM) for motion control. The DRV8213 integrates a current sensing system and implements closed-loop PID current control. Communication is achieved via the SPI protocol, with CRC verification, supporting a maximum communication frequency of 1 kHz. The system can drive four motors with an adjustable voltage range of 3V to 12V. Additionally, to ensure the safety of movement, a low-pass filter is incorporated in the communication process to provide disconnection protection.

IV. ANALYSIS

A. Kinematics and Dynamics

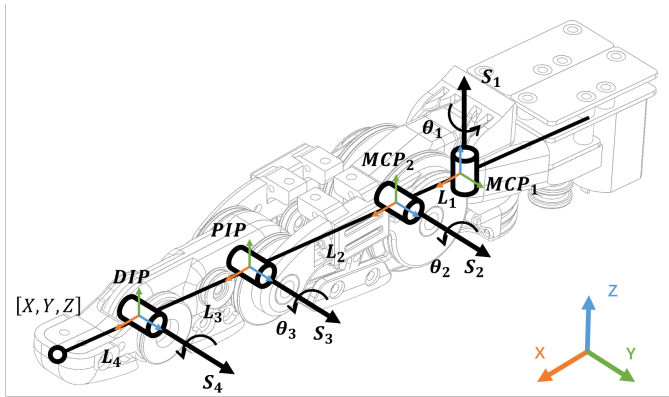


Fig. 8. Kinematic Structure of a Single Finger

As shown in Fig. 8, based on the structure above, we define the forward kinematic model of a single finger as follows

$$T(\theta) = \prod_{i=1}^3 e^{[S_i]\theta_i} M. \quad (1)$$

After locking the DIP joint, the correspondence between the fingertip coordinates and the joint angles of the finger can be obtained through forward kinematics

$$\begin{cases} Xs_1 - Yc_1 = 0 \\ (L_2 + L_3c_3)s_2 + L_3s_3c_2 - Z = 0 \\ (\sqrt{X^2 + Y^2} - L_1)^2 + Z^2 - L_2^2 - L_3^2 - 2L_2L_3c_3 = 0 \end{cases} \quad (2)$$

The position of the joint is independently driven by the motors corresponding to the previously discussed configurations, and the relationship between joint torque and the torque output of the corresponding motors is analyzed. As show in Fig. 2 and Fig. 4, The MCP joint is driven by the motor located in the palm region, while the PIP joint is directly driven by the motor in the forearm. Therefore, the motor torque output relationship corresponding to the finger joints is as follows

$$\begin{cases} M_{MCP1} = \frac{R_{MCP1}}{r_{palm}} (\tau_{palm1} + \tau_{palm2}) \\ M_{MCP2} = \frac{R_{MCP2}}{r_{palm}} (\tau_{palm1} - \tau_{palm2}) \\ M_{PIP} = \frac{R_{PIP}}{r_{arm}} \tau_{arm} \end{cases} \quad (3)$$

B. Control Strategy

The control strategy for the entire hand is shown in the Fig. 9. Initially, the position difference is calculated using the position data obtained from the position sensors, and the desired motion information for each motor is determined through a dynamic model. The target current for each motor is then calculated using a PID controller. The motor current control loop is integrated into the motor control board, where the PID loop regulates the current output to control the torque. A low-pass filter is also designed to protect the system from damage due to disconnection.

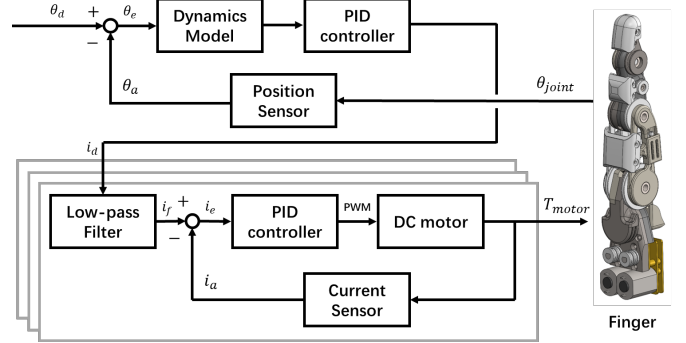


Fig. 9. Control Block Diagram of a Single Finger

V. RESULT

A. Performance of Single Finger

To evaluate the mechanical characteristics of fingertip compression, a dedicated testing platform was developed. As illustrated in Fig. 10, a three-axis force sensor (ZNSW-F) was rigidly mounted on the experimental platform to capture multidirectional force signals. Subjects were instructed to apply the maximum vertical compressive force using their index finger under controlled conditions. The force distribution across orthogonal axes is quantified in Fig. 11. The maximum compressive force along the Z-axis reached 11 N, highlighting the dominant loading direction during fingertip compression. The design speed of the finger joint movement is approximately 30 rpm, and the design load for the whole hand grip is around 10 kg.

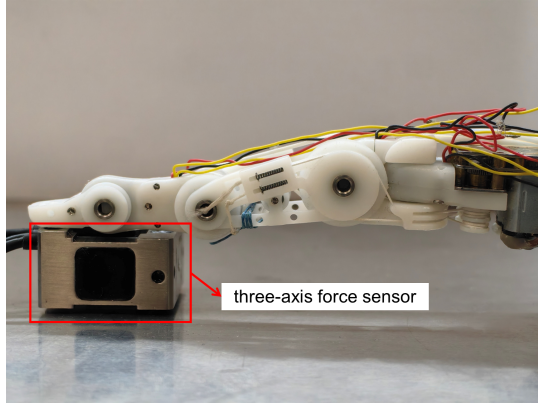


Fig. 10. Testing Platform for contact force measurement.

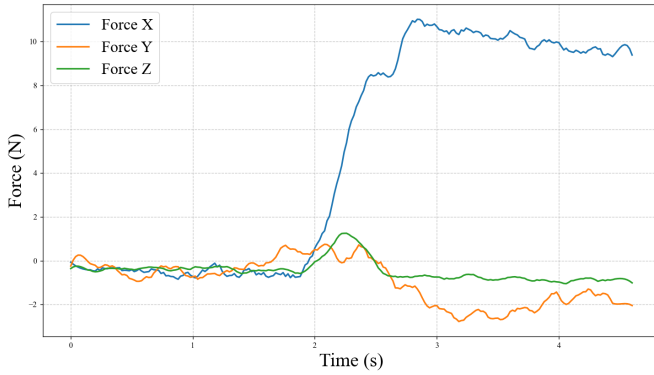


Fig. 11. Contact force of single finger

TABLE II
FINGER JOINT MOTION AND LENGTH

Joint	Range of rotation	Phalange Length
MCP-1	-30°-30°	16mm
MCP-2	0°-90°	32mm
PIP	0°-90°	24mm
DIP (Optional)	0°-90°	20mm

B. Workspace

Table II shows the key parameters and range of motion of a single finger. Fig. 12 illustrates the total workspace of each fingertip center point of the IRMV Hand. Each finger's workspace is color-coded in the Fig. 12, with different colors representing the motion space of each finger. The total volume of the workspace for each finger is 99 cm³, indicating the extent of motion flexibility provided by the system.

C. Object Grasping

This study systematically validates the manipulation capability of the IRMV Hand using the Grasp Taxonomy benchmark established by Feix et al. [27]. This benchmark evaluates the hand's adaptability to geometrically diverse objects by defining grasping paradigms under varying geometric and force constraints. As shown in Fig. 13, the IRMV hand successfully achieved 33 distinct grasp types from the taxonomy, encompassing power grasps, precision grasps, and hybrid

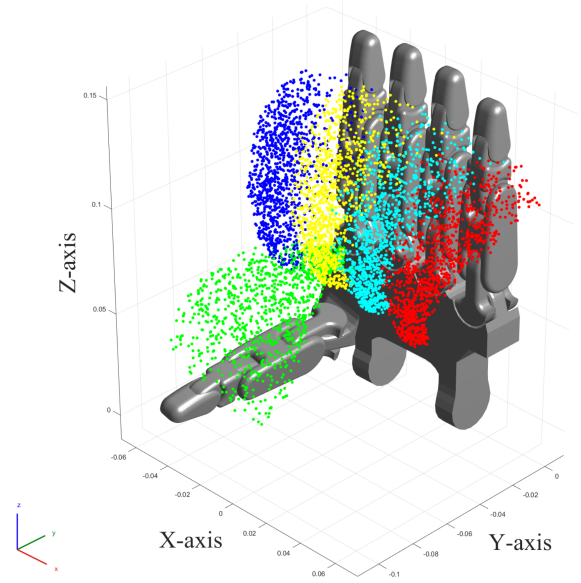


Fig. 12. Workspace with Colored Points of the IRMV Hand.

grasp modes. This empirically demonstrates its versatility and robustness in multi-scale object manipulation tasks.

The robotic hand was able to securely grasp these objects using different postures. The images highlight the hand's capability to handle both symmetric and irregularly shaped objects, emphasizing its dexterity. The results confirm that the robotic hand can reliably grasp objects with a wide range of shapes, demonstrating its potential for numerous automation and robotic manipulation applications.

VI. CONCLUSION

This paper proposes a novel bionic hand structure that overcomes the limitations of traditional bionic hand designs, where the power sources are typically confined to the fingers, palm, or forearm. It addresses the issues of low power density and bulky forearm configurations. By adopting a distributed drive design, motors are strategically placed in the forearm and palm, optimizing space utilization while achieving a compact overall structure. The design offers 15 DoFs, making it closer to the physiological structure of the human hand. This design not only significantly improves the power density and motion performance of the bionic hand but also provides a new perspective for the development of high-performance bionic hands in the future.

Our next step involves expanding the sensory tasks of the bionic fingers, including the development of tendon tension sensors and tactile skin sensors. We also plan to improve the design of the wrist mechanism, with the goal of achieving more dexterous hand operation tasks.

REFERENCES

- [1] C. Piazza, G. Grioli, M. Catalano, and A. Bicchi, "A century of robotic hands," vol. 2, no. 1, pp. 1–32. [Online]. Available: <https://www.annualreviews.org/doi/10.1146/annurev-control-060117-105003>

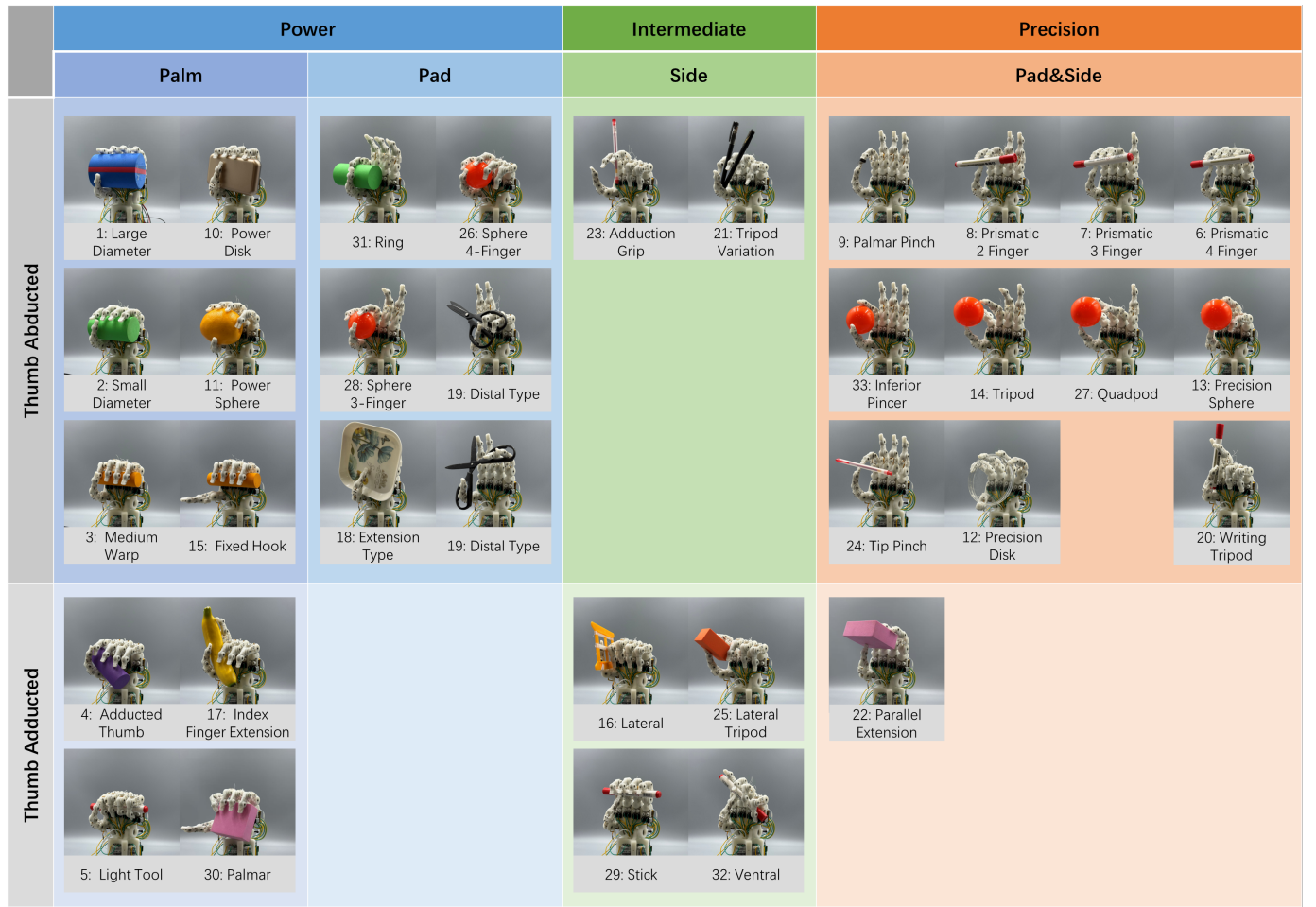


Fig. 13. GRASP taxonomy on the IRMV Hand.

- [2] V. P. Nguyen, S. B. Dhyam, V. Mai, B. S. Han, and W. T. Chow, "Bioinspiration and biomimetic art in robotic grippers," vol. 14, no. 9, p. 1772. [Online]. Available: <https://www.mdpi.com/2072-666X/14/9/1772>
- [3] H. P. Von Schroeder and M. J. Botte, "Anatomy and functional significance of the long extensors to the fingers and thumb," vol. 383, pp. 74–83. [Online]. Available: <http://journals.lww.com/00003086-200102000-00010>
- [4] S. Suresh, H. Qi, T. Wu, T. Fan, L. Pineda, M. Lambeta, J. Malik, M. Kalakrishnan, R. Calandra, M. Kaess, J. Ortiz, and M. Mukadam. Neural feels with neural fields: Visuo-tactile perception for in-hand manipulation. [Online]. Available: <http://arxiv.org/abs/2312.13469>
- [5] J.-H. Bae, S.-W. Park, J.-H. Park, M.-H. Baeg, D. Kim, and S.-R. Oh, "Development of a low cost anthropomorphic robot hand with high capability," in *2012 IEEE/RSJ International Conference on Intelligent Robots and Systems*. Vilamoura-Algarve, Portugal: IEEE, 2012, pp. 4776–4782.
- [6] D.-H. Lee, J.-H. Park, S.-W. Park, M.-H. Baeg, and J.-H. Bae, "Kitech-hand: A highly dexterous and modularized robotic hand," *IEEE/ASME Transactions on Mechatronics*, vol. 22, no. 2, pp. 876–887, 2017.
- [7] "Allegro hand," <https://www.wonikrobotics.com/research-robot-hand>.
- [8] K. Shaw, A. Agarwal, and Deepak Pathak, "Leap hand: Low-cost, efficient, and anthropomorphic hand for robot learning," in *Robotics: Science and Systems XIX*. Robotics: Science and Systems Foundation, 2023.
- [9] H. Kawasaki, T. Komatsu, and K. Uchiyama, "Dexterous anthropomorphic robot hand with distributed tactile sensor: Gifu hand ii," *IEEE-ASME TRANSACTIONS ON MECHATRONICS*, vol. 7, no. 3, pp. 296–303, 2002.
- [10] H. Hu, Z. Xie, Y. Liu, Y. Liu, G. Yang, J. Xia, and H. Liu, "A variable stiffness actuation based robotic hand designed for interactions," *IEEE-ASME TRANSACTIONS ON MECHATRONICS*, vol. 29, no. 1, pp. 249–259, 2024.
- [11] W. Li, L. Jiang, M. Cheng, J. Dai, S. Fan, and H. Liu, "Multisensory integrated dexterous finger with coupled-adaptive features," *IEEE-ASME TRANSACTIONS ON MECHATRONICS*, 2024.
- [12] U. Kim, D. Jung, H. Jeong, J. Park, H.-M. Jung, J. Cheong, H. R. Choi, H. Do, and C. Park, "Integrated linkage-driven dexterous anthropomorphic robotic hand," *Nature Communications*, vol. 12, no. 1, p. 7177, 2021.
- [13] A. D. Deshpande, Z. Xu, M. J. Vande Weghe, B. H. Brown, J. Ko, L. Y. Chang, D. D. Wilkinson, S. M. Bidic, and Y. Matsuoka, "Mechanisms of the anatomically correct testbed hand," *IEEE-ASME TRANSACTIONS ON MECHATRONICS*, vol. 18, no. 1, pp. 238–250, 2013.
- [14] "Shadowhand," <https://ninjatek.com/shop/edge/>.
- [15] H. Liu, P. Meusel, G. Hirzinger, M. Jin, Y. Liu, and Z. Xie, "The modular multisensory dlr-hit-hand: Hardware and software architecture," *IEEE-ASME TRANSACTIONS ON MECHATRONICS*, vol. 13, no. 4, pp. 461–469, 2008.
- [16] M. Chalon, M. Grebenstein, T. Wimböck, and G. Hirzinger, "The thumb: guidelines for a robotic design," in *2010 IEEE/RSJ International Conference on Intelligent Robots and Systems*. Taipei: IEEE, 2010, pp. 5886–5893.
- [17] W. Friedl, M. Chalon, J. Reinecke, and M. Grebenstein, "Fas a flexible antagonistic spring element for a high performance over," in *2011 IEEE/RSJ International Conference on Intelligent Robots and Systems*. San Francisco, CA: IEEE, 2011, pp. 1366–1372.
- [18] M. Grebenstein, A. Albu-Schaffer, T. Bahlis, M. Chalon, O. Eiberger, W. Friedl, R. Gruber, S. Haddadin, U. Hagn, R. Haslinger, H. Hoppner, S. Jorg, M. Nickl, A. Nothelfer, F. Petit, J. Reill, N. Seitz, T. Wimböck, S. Wolf, T. Wusthoff, and G. Hirzinger, "The dlr hand arm system," in *2011 IEEE International Conference on Robotics and Automation*. Shanghai, China: IEEE, 2011, pp. 3175–3182.
- [19] W. Friedl, M. Chalon, J. Reinecke, and M. Grebenstein, "frcef: The new friction reduced and coupling enhanced finger for the awiwi hand," in

2015 IEEE-RAS 15th International Conference on Humanoid Robots (Humanoids). Seoul, South Korea: IEEE, 2015, pp. 140–147.

- [20] L. B. Bridgwater, C. A. Ihrke, M. A. Diftler, M. E. Abdallah, N. A. Radford, J. M. Rogers, S. Yayathi, R. S. Askew, and D. M. Linn, “The robonaut 2 hand - designed to do work with tools,” in *2012 IEEE International Conference on Robotics and Automation*. St Paul, MN, USA: IEEE, 2012, pp. 3425–3430.
- [21] F. Lotti, P. Tiezzi, G. Vassura, L. Biagiotti, G. Palli, and C. Melchiorri, “Development of ub hand 3: Early results,” in *Proceedings of the 2005 IEEE International Conference on Robotics and Automation*. Barcelona, Spain: IEEE, 2005, pp. 4488–4493.
- [22] C. Melchiorri, G. Palli, G. Berselli, and G. Vassura, “Development of the ub hand iv: Overview of design solutions and enabling technologies,” *IEEE Robotics & Automation Magazine*, vol. 20, no. 3, pp. 72–81, 2013.
- [23] Y.-J. Kim, J. Yoon, and Y.-W. Sim, “Fluid lubricated dexterous finger mechanism for human-like impact absorbing capability,” *IEEE Robotics and Automation Letters*, vol. 4, no. 4, pp. 3971–3978, 2019.
- [24] S. Min and S. Yi, “Development of cable-driven anthropomorphic robot hand,” *IEEE Robotics and Automation Letters*, vol. 6, no. 2, pp. 1176–1183, 2021.
- [25] Y.-J. Kim, Y. Lee, J. Kim, J.-W. Lee, K.-M. Park, K.-S. Roh, and J.-Y. Choi, “Roboray hand: A highly backdrivable robotic hand with sensorless contact force measurements,” in *2014 IEEE International Conference on Robotics and Automation (ICRA)*. Hong Kong, China: IEEE, 2014, pp. 6712–6718.
- [26] Z. K. Weng. Bidexhand: Design and evaluation of an open-source 16-dof biomimetic dexterous hand. [Online]. Available: <http://arxiv.org/abs/2504.14712>
- [27] T. Feix, J. Romero, H.-B. Schmiedmayer, A. M. Dollar, and D. Kragic, “The grasp taxonomy of human grasp types,” vol. 46, no. 1, pp. 66–77. [Online]. Available: <http://ieeexplore.ieee.org/document/7243327/>
- [28] G. Palli, U. Scarcia, C. Melchiorri, and G. Vassura, “Development of robotic hands: The ub hand evolution,” in *2012 IEEE/RSJ International Conference on Intelligent Robots and Systems*. Vilamoura-Algarve, Portugal: IEEE, 2012, pp. 5456–5457.
- [29] J. Rastegar and B. Fardanesh, “Manipulation workspace analysis using the monte carlo method,” *Mechanism and Machine Theory*, vol. 25, no. 2, pp. 233–239, 1990.
- [30] H. Li, C. J. Ford, M. Bianchi, M. G. Catalano, E. Psomopoulou, and N. F. Lepora, “Brl/pisa/iit softthand: A low-cost, 3d-printed, underactuated, tendon-driven hand with soft and adaptive synergies,” vol. 7, no. 4, pp. 8745–8751. [Online]. Available: <https://ieeexplore.ieee.org/document/9813397/>



Yifei Yu enrolled in the undergraduate program in Automation Engineering at Shanghai university of electric power in 2023

His research interests include mechanism design and robotics.



Yixuan Zhou received the B.Eng. degree in Mechatronics Engineering in 2018, from Beijing Institute of Technology, Beijing, China, where he also received an M.Eng. degree in Mechanical Engineering in 2021 too. He is currently working towards the Ph.D. degree in Control Science and Engineering in Shanghai Jiao Tong University, Shanghai, China.

His current research interests include vision-based manipulation, visual servoing and trajectory planning.



Xiaohan Zhu received the B.S. degree in automation from the Harbin Institute of Technology (HIT), Harbin, China, in 2023. He is currently working toward the M.S. degree in control technology and control engineering with the Department of Automation, Shanghai Jiao Tong University.

His research interests include soft robots, humanoid robots, and surgical robots.



Haoqi Han received the B.Eng. degree in Mechatronics Engineering in 2018, from Beijing Institute of Technology, Beijing, China. He is currently working towards the Ph.D. degree in Computer Science and Engineering in Shanghai Jiao Tong University, Shanghai, China.

His current research interests include biomimetic mechanisms.



Yi Yang enrolled in the undergraduate program in Engineering Mechanics at Shanghai Jiao Tong University in 2023.

His research interests include dexterous hand and robotics.



Hesheng Wang (SM'15) received the B.Eng. degree in electrical engineering from the Harbin Institute of Technology, Harbin, China, in 2002, and the M.Phil. and Ph.D. degrees in automation and computer-aided engineering from The Chinese University of Hong Kong, Hong Kong, in 2004 and 2007, respectively. He is currently a Distinguished Professor with the Department of Automation, Shanghai Jiao Tong University, Shanghai, China. His current research interests include visual servoing, intelligent robotics, computer vision, and autonomous driving.

Dr. Wang is an Associate Editor of Robotic Intelligence and Automation and the International Journal of Humanoid Robotics, a Senior Editor of the IEEE/ASME Transactions on Mechatronics, an Editor-in-chief of Robot Learning. He served as an Associate Editor of the IEEE Transactions on Robotics from 2015 to 2019, an IEEE Transactions on Automation Science and Engineering from 2021 to 2023, a Technical Editor of the IEEE/ASME Transactions on Mechatronics from 2020 to 2023, an Editor of Conference Editorial Board (CEB) of IEEE Robotics and Automation Society from 2022 to 2024. He was the General Chair of IEEE ROBIO 2022 and IEEE RCAR 2016, and the Program Chair of the IEEE ROBIO 2014 and IEEE/ASME AIM 2019. He will be the General Chair of IEEE/RSJ IROS 2025.